

LDPC Decoding Over Non-Binary Queue-Based Burst Noise Channels

Pedro Melo, Cecilio Pimentel, *Senior Member, IEEE*, and Fady Alajaji, *Senior Member, IEEE*

Abstract—Iterative decoding based on the sum-product algorithm (SPA) is examined for sending low-density parity check (LDPC) codes over a discrete non-binary queue-based Markovian burst noise channel. This channel model is adopted due to its analytical tractability and its recently demonstrated capability in accurately representing correlated flat Rayleigh fading channels under antipodal signaling and either hard or soft output quantization. SPA equations are derived in closed-form for this model in terms of its parameters. It is then numerically observed that potentially large coding gains can be realized with respect to the Shannon limit by exploiting channel memory as opposed to ignoring it via interleaving. Finally, the LDPC decoding performance under both matched and mismatched decoding regimes is evaluated. It is shown that the Markovian model provides noticeable gains over channel interleaving and that it can effectively capture the underlying fading channels behavior when decoding LDPC codes.

Index Terms—Burst Noise, finite-state Markov channels, modeling correlated Rayleigh fading channels, Shannon limit, matched and mismatched decoding, hard and soft-decision demodulation, channel interleaving, low-density parity-check codes, iterative decoding.

I. INTRODUCTION

A Discrete (binary-input 2^q -ary output) burst noise channel model was recently introduced in [1], called the non-binary noise discrete channel (NBND), to model fading channels with memory and soft-decision information. The channel's 2^q -ary output process can be written as an explicit function of the binary input and 2^q -ary noise processes. We refer to as NBND-QB the NBND with the non-binary queue-based (QB) M -th order Markov noise process with $2^q + 2$ independent parameters proposed in [1]. The NBND-QB has a small number of parameters (as typically q is not greater than three) and is mathematically tractable, featuring desirable statistical and information-theoretic properties (such as symmetry, Markovian noise structure and closed-form expressions for its block distribution) unlike the classical burst-noise Gilbert-Elliott channel (GEC) and other finite-state Markov channel (FSMC) models in the literature (which typically exhibit a hidden Markovian noise structure; e.g. see [2], [3], [4]). The NBND-QB can effectively model (in terms of replicating channel capacity and noise autocorrelation function) a discrete fading channel (DFC) composed of a binary phase-shift keying modulator, a time-correlated flat Rayleigh

fading channel with Clarke's autocorrelation function and a q -bit (uniform) scalar soft-quantized coherent demodulator [1]. It also subsumes as a special case (when $q = 1$) the binary-input binary-output QB channel [5] shown in [6] to accurately represent (also in terms of capacity and noise autocorrelation function) the DFC under hard-decision demodulation. In [7], it is further demonstrated that the NBND-QB is a good fit for the DFC in terms of signal-to-distortion fidelity under both channel optimized quantization and scalar quantization with sequence maximum a posteriori detection.

The aim of this correspondence is to examine the potential theoretical channel coding gains achievable via the NBND-QB model vis-a-vis its corresponding (ideally interleaved) memoryless counterpart as well as examine the NBND-QB's modeling effectiveness of approximating the behavior of correlated fading channels when decoding practical powerful low-density parity check (LDPC) codes. Several authors studied the design of a belief propagation scheme for joint decoding and channel state estimation of LDPC codes over FSMC's [8]-[14]. The decoder uses a factor graph with variable nodes related to the code constraints as well as to the FSMC structure. These works are typically concentrated on a special case of a binary (binary-input binary-output) FSMC, which, unlike the NBND-QB model, do not accommodate non-binary output alphabets for capturing the soft-decision information of underlying soft-output quantized fading channels. Moreover, in these works, the channel type that corrupts the codeword is the same one used in the factor graph at the decoder (which results in a matched decoder). Other related works include the development of efficient iterative detection and decoding methods for coherent and non-coherent fading channels with memory; see [15], [16] and the references therein.

The contribution of this correspondence is threefold. First, we specialize the sum-product algorithm (SPA) to the NBND-QB channel, exploiting its mathematical tractability, to derive closed-form equations for the messages passed through the factor graph when decoding LDPC codes over this channel. Then, we study the potential coding gain in terms of the Shannon limit provided by the NBND-QB over the standard delay-prone approach of interleaving the channel to spread its error bursts over the set of received codewords and render its memoryless with respect to the decoder. Finally, we study the accuracy of the NBND-QB in approximating the DFC from a new perspective (not considered in [1], [8]-[14]). Specifically, we investigate the LDPC performance when the true underlying channel is the DFC while the decoder uses an NBND-QB channel chosen to fit the DFC by minimizing the Kullback-Leibler divergence rate between the channel noise

P. Melo and C. Pimentel are with the Department of Electronics and Systems, Federal University of Pernambuco, Recife, PE, 50711-970, Brazil, email: cecilio@ufpe.br, pmelo@hotmail.com.

F. Alajaji is with the Department of Mathematics and Statistics, Queen's University, Kingston, ON K7L 3N6, Canada, email: fady@mast.queensu.ca.

This work was supported in part by NSERC of Canada and CNPq of Brazil.

sources as in [1]. We show that this mismatch decoding is capable of outperforming the fully-interleaved (memoryless) DFC; this demonstrates that the finite-memory NBNDQ-B channel with low number of parameters can be effectively used to exploit the fading statistical dependence of the DFC. Moreover, this study illustrates the practicality of modeling the DFC via the NBNDQ-B in terms of iterative channel decoding performance.

II. THE NBNDQ-B MODEL

Let $\{X_k\}$ be the binary-input process and $\{Y_k\}$ be the 2^q -ary output process (over the alphabet $\{0, 1, \dots, 2^q - 1\}$) of the NBNDQ-B channel. Its 2^q -ary noise process $\{Z_k\}$ is independent from the input process and is given by [1] $Z_k = [Y_k - (2^q - 1)X_k]/(-1)^{X_k}$. The channel noise is an M -th order stationary ergodic Markov process with state $S_k = (Z_{k-1}, Z_{k-2}, \dots, Z_{k-M})$ and is generated based on the following ball sampling mechanism. First, one of two parcels (an urn containing balls with 2^q different colors representing noise symbols and a queue of size M are selected with probability distribution $\{\varepsilon, 1 - \varepsilon\}$). If the urn is selected, the model generates a noise symbol $Z_k = j$ with probability ρ_j , $j \in \{0, 1, \dots, 2^q - 1\}$. If the queue is selected, a noise symbol Z_k is an entry from the queue selected randomly with a probability distribution that depends on M and a bias parameter $\alpha \geq 0$. The entries of the queue are shifted to the right and Z_k becomes the first entry in the queue. The QB noise parameters are the distribution $(\rho_0, \dots, \rho_{2^q-1})$ and the triplet (M, α, ε) . The state stationary distribution vector $\boldsymbol{\Pi} = [\pi_{z^M}]$ given by [1, Eq. (18)] (each state is indexed by an M -tuple $z^M = (z_0, z_1, \dots, z_{M-1})$) and the noise correlation coefficient is given by

$$\text{Cor}_{\text{QB}} = \frac{\mathbf{E}[Z_k Z_{k+1}] - \mathbf{E}[Z_k]^2}{\text{Var}(Z_k)} = \frac{\frac{\varepsilon}{M-1+\alpha}}{1 - (M-2+\alpha)\frac{\varepsilon}{M-1+\alpha}} \quad (1)$$

where $\mathbf{E}[\cdot]$ denotes expected value and $\text{Var}(Z_k)$ denotes the variance of Z_k . Given a DFC with fixed parameters (signal-to-noise ratio, SNR, normalized maximum Doppler frequency, $f_D T$, soft-decision resolution, q , and quantization step, δ), we fit the NBNDQ-B by first matching the one-dimensional probability distribution $\rho_j = P_{\text{DFC}}(y|x)$, where $j = (y - (2^q - 1)x)/(-1)^x$ and $P_{\text{DFC}}(y|x)$ is given by [1, Eq. (3)]. The remaining QB parameters (M, α, ε) are obtained by minimizing the Kullback-Leibler divergence rate between the DFC and QB noise processes (see details of the parameterization procedure in [1]). This minimization assures that the n -order probability distributions $P_{\text{QB}}(z^n)$ and $P_{\text{DFC}}(z^n)$ of both processes are statistically close for large blocklengths. While $P_{\text{QB}}(z^n)$ has a closed-form expression in terms of the QB parameters, $P_{\text{DFC}}(z^n)$ is obtained by computer simulations of time-correlated Rayleigh fading samples using the sum-of-sinusoids method [17]. The samples at the output of the matched filter are compared with the thresholds of a uniform quantizer, where the optimum quantization step δ is selected to maximize a lower bound on the Shannon capacity of the underlying DFC. In Section IV, the similarity between these

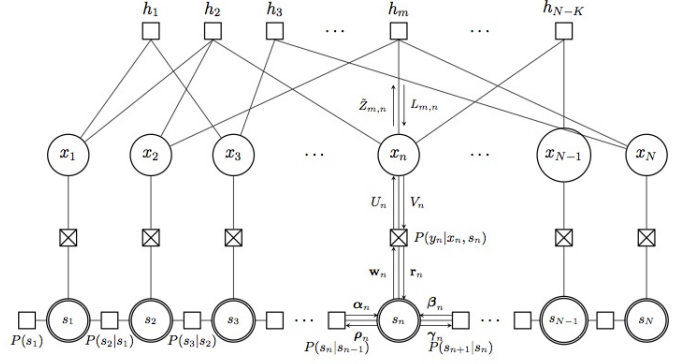


Fig. 1. Factor graph used to decode an LDPC over an FSMC.

two channels is investigated in terms of the system's end-to-end bit error rate (BER) when decoding LDPC codes.

III. LDPC DECODING APPLIED TO THE NBNDQ-B

Let $\mathbf{x} = (x_1, \dots, x_N)$ be a codeword encoded by an (N, K) LDPC code. When this codeword is transmitted through an FSMC, the joint probability density function of the transmitted codeword, state sequence $\mathbf{s} = (s_1, \dots, s_N)$ and received word $\mathbf{y} = (y_1, \dots, y_N)$ is [12]

$$P(\mathbf{x}, \mathbf{s}, \mathbf{y}) = P_S(s_1) \prod_{i=1}^{N-1} P_{S_{i+1}|S_i}(s_{i+1}|s_i) \times \prod_{i=1}^N P_{Y_i|X_i, S_i}(y_i|x_i, s_i) h(\mathbf{x}) \quad (2)$$

where $h(\mathbf{x})$ is the characteristic function of an error-correcting code [18]. From (2), it is possible to obtain the factor graph presented in Fig. 1 [12], [13]. This graph may be decomposed in two subgraphs, one which involves variables and functions related to the code, the *code graph*, and one which involves variables and functions related to the channel dynamics, the *channel graph*. We denote the set of bits that participate in the code constraint m as $\mathcal{N}(m)$ and the set of code constraints in which bit n participates as $\mathcal{M}(n)$. We also denote as $\mathcal{N}(m) \setminus n$ the set $\mathcal{N}(m)$ with bit n excluded and $\mathcal{M}(n) \setminus m$ the set $\mathcal{M}(n)$ with code constraint m excluded.

We present next the SPA [18] messages passed through the factor graph in Fig. 1 when the channel model used at the decoder is the NBNDQ-B (the SPA messages for the GEC are treated in [12], [13]). If the channel that corrupts a codeword is the DFC, it is assumed that it is modeled by means of an NBNDQ-B. The decoding procedure is as follows.

- **Initialization:** We obtain for $n = 1$ to N :

$$\alpha_n(z^M) = \beta_n(z^M) = \pi_{z^M},$$

$$\pi_{z^M} = \frac{\prod_{\ell=0}^{2^q-1} \prod_{m=0}^{\xi_\ell-1} \left((1-\varepsilon)\rho_\ell + m \frac{\varepsilon}{M-1+\alpha} \right)}{\prod_{k=0}^{M-1} \left((1-\varepsilon) + k \frac{\varepsilon}{M-1+\alpha} \right)}$$

where $\xi_\ell = \sum_{k=0}^{M-1} \delta_{z_k, \ell}$ and

$$\delta_{i,j} = \begin{cases} 1, & \text{if } i = j \\ 0, & \text{otherwise.} \end{cases}$$

Compute $\bar{y}_n = 2^q - 1 - y_n$, and for $n = 1$ to N , the log-likelihood (LLR) U_n 's are the messages from the channel subgraph to the associated bit nodes. It is known that the LLR messages offer implementation advantages in the messages exchanged in the code subgraph. The message U_n is given by (4) at the top of the next page, where the derivation of (4) from (3) is based on the QB noise generation mechanism. Moreover, set $\tilde{Z}_{m,n} = U_n$, for $m \in \mathcal{N}(n)$.

• **Iterative processing**

- *Processing in the code subgraph*

- 1) For $m = 1$ to $N - K$ and $n \in \mathcal{N}(m)$, the message $\{L_{m,n}\}$ passed from the code constraint m to bit node n is calculated according to the ‘‘tanh’’ rule

$$L_{m,n} = 2 \arctan \left(\prod_{n' \in \mathcal{N}(m) \setminus n} \tanh \left(\frac{1}{2} \tilde{Z}_{m,n'} \right) \right).$$

- 2) For $n = 1$ to N , the message passed from the the code graph to the channel graph is $V_n = \sum_{m \in \mathcal{M}(n)} L_{m,n}$ with probabilistic representation

$$v_n(0) = e^{V_n} / (1 + e^{V_n}), \quad v_n(1) = 1 / (1 + e^{V_n}).$$

- 3) *Variable node update*

- a) For $n = 1$ to N and for $m \in \mathcal{M}(n)$: $\tilde{Z}_{m,n} = U_n + \sum_{m' \in \mathcal{M}(n) \setminus m} L_{m',n}$.

- *Processing in the channel subgraph*

The messages passed in the channel subgraph are 2^{qM} -dimensional vectors, $\mathbf{r}_n = [r_n(z^M)]$, $\mathbf{w}_n = [w_n(z^M)]$, $\boldsymbol{\alpha}_n = [\alpha_n(z^M)]$, $\boldsymbol{\rho}_n = [\rho_n(z^M)]$, $\boldsymbol{\beta}_n = [\beta_n(z^M)]$, $\boldsymbol{\gamma}_n = [\gamma_n(z^M)]$. The entries of these vectors are as follows.

- 1) For $n = 1$ to N the messages $r_n(z^M)$ are given by (5) at the top of the next page.

- 2) The messages leaving a state node are:

$$\begin{cases} \gamma_n(z^M) = \alpha_n(z^M)r_n(z^M), & \text{for } n = 1 \text{ to } N - 1 \\ \rho_n(z^M) = \beta_n(z^M)r_n(z^M), & \text{for } n = 2 \text{ to } N. \end{cases}$$

- 3) The messages $\alpha_n(z^M)$, for $n = 2$ to N , and $\beta_n(z^M)$, for $n = 1$ to $N - 1$, are given by (6) and (7) at the top of the next page.

- 4) For $n = 1$ to $N - 1$: $w_n(z^M) = \alpha_n(z^M)\beta_n(z^M)$.

For $n = 1$ to N , the messages U_n are given by (8) at the top of the next page.

There are several ways to organize the message passing schedule when running SPA, as described in [13]. We choose a schedule that performs one iteration on the code subgraph and then one iteration on the channel subgraph, giving an equal schedule time to each subgraph.¹ In the channel subgraph,

all $\boldsymbol{\alpha}_n$ vectors are first passed in a forward manner and all messages are stored in each state node. When the N -th state node is reached, all $\boldsymbol{\beta}_n$ vectors are calculated in a backward manner, yielding the \mathbf{w}_n and U_n messages, so that $\boldsymbol{\beta}_n$ does not need to be stored.

IV. RESULTS

A. Shannon Limit

For a system using an error-correcting code with rate $r = K/N$, the optimal performance theoretically achievable or Shannon limit (SL), established by the lossy joint source-channel coding Theorem (e.g, see [19, Theorem 10.4.1], [20, Section V.B]), yields the lowest channel SNR for which decoding can be realized at a target end-to-end BER P_e . To calculate SL for an NBNDQ-QB channel with $q = 1$,² we first fix its parameters (ε, α, M) and the remaining parameter ρ_1 is given via [1, Eq. (3)] in terms of SNR as the one-dimensional channel error rate of the underlying DFC. Then for a given target BER P_e , we determine the SNR value that satisfies

$$C(\rho_1) = r [1 + P_e \log_2 P_e + (1 - P_e) \log_2 (1 - P_e)] =: r R(P_e)$$

where channel capacity $C = C(\rho_1)$ is calculated using [5, Eq. (24)]. This means that if data is sent at a rate $r < C/R(P_e)$ then a probability of error as low as P_e can be achieved.

To analyze the potential coding gain provided by the NBNDQ-QB, we study the SL behavior for this channel under a fixed correlation coefficient (Cor_{QB}). For a given value of M , say $M = 2, 4, 6, 8$, we use $\alpha = 1$ and find ε using (1) such that $\text{Cor}_{\text{QB}} = 0.5$. The SL curves (P_e versus SNR) for the NBNDQ-QB channels with increasing values of the memory order M are presented in Fig. 2. We observe impressive coding gains even for small values of M . For example, for the simplest model presented with $M = 2$, a gain superior to 4 dB is obtained with respect to the SL of the binary symmetric channel (BSC) which corresponds to the perfectly interleaved channel. The gain reaches 7.5 dB for $M = 8$.

We next consider NBNDQ-QB channels that approximate the DFC with fixed parameters. The QB parameters α and ε are obtained by the minimization of the Kullback-Leibler divergence rate for selected values of M [1]. The SL curves obtained for NBNDQ-QB channels with increasing values of M that approximate a DFC with $f_{DT} = 0.005$, SNR = 1 dB, and $q = 1$ are shown in Fig. 3. We observe a coding gain up to 1.07 dB for the case $M = 22$.

B. Matched and Mismatched Decoding of LDPC Codes

In order to evaluate the system's end-to-end BER obtained by modeling the DFC through the NBNDQ-QB, we implement the iterative LDPC decoder presented in Section III with at most 200 iterations. We use a regular LDPC code with parameters $(N = 15000, K = 7500)$ with column degree $d_v = 3$. The parity-check matrix \mathbf{H} is generated using the PEG algorithm [21].

¹This schedule provides a good trade-off between convergence speed and performance [13].

²We only evaluate SL for $q = 1$, which corresponds to hard-decision demodulation in the underlying DFC, since the NBNDQ does not admit a closed-form capacity expression as a function of its parameters for $q > 1$ [1].

$$\begin{aligned}
U_n &= \ln \left(\frac{\sum_{z^M} P_{QB}(y_n|x_n=0, s_n=z^M) \pi_{z^M}}{\sum_{z^M} P_{QB}(y_n|x_n=1, s_n=z^M) \pi_{z^M}} \right) \\
&= \ln \left(\frac{\sum_{z^M} P_{QB}(z_n=y_n|s_n=z^M) \pi_{z^M}}{\sum_{z^M} P_{QB}(z_n=\bar{y}_n|s_n=z^M) \pi_{z^M}} \right) \tag{3}
\end{aligned}$$

$$= \ln \left(\frac{\left((1-\varepsilon)\rho_{y_n} + \frac{\varepsilon}{M-1+\alpha} \sum_{z^M} \left(\sum_{\ell=1}^{M-1} \delta_{y_n, z_\ell} + \alpha \delta_{y_n, z_0} \right) \pi_{z^M} \right)}{\left((1-\varepsilon)\rho_{\bar{y}_n} + \frac{\varepsilon}{M-1+\alpha} \sum_{z^M} \left(\sum_{\ell=1}^{M-1} \delta_{\bar{y}_n, z_\ell} + \alpha \delta_{\bar{y}_n, z_0} \right) \pi_{z^M} \right)} \right) \tag{4}$$

$$\begin{aligned}
r_n(z^M) &= \sum_{x_n=0}^1 P_{QB}(y_n|x_n, z^M) v_n(x_n) \\
&= P_{QB}(z_n=y_n|z^M) v_n(0) + P_{QB}(z_n=\bar{y}_n|z^M) v_n(1) \\
&= \left[\left(\sum_{\ell=1}^{M-1} \delta_{y_n, z_\ell} + \alpha \delta_{y_n, z_0} \right) \frac{\varepsilon}{M-1+\alpha} + (1-\varepsilon)\rho_{y_n} \right] v_n(0) + \\
&\quad + \left[\left(\sum_{\ell=1}^{M-1} \delta_{\bar{y}_n, z_\ell} + \alpha \delta_{\bar{y}_n, z_0} \right) \frac{\varepsilon}{M-1+\alpha} + (1-\varepsilon)\rho_{\bar{y}_n} \right] v_n(1). \tag{5}
\end{aligned}$$

$$\begin{aligned}
\alpha_n(z^M) &= \sum_{s_{n-1}} P_{QB}(s_n=z^M|s_{n-1}) \gamma_{n-1}(s_{n-1}) \\
&= \sum_{i=0}^{2^q-1} \left[\left(\alpha \delta_{z^M, i} + \sum_{\ell=1}^{M-1} \delta_{z^M, z_{M-\ell}} \right) \frac{\varepsilon}{M-1+\alpha} + (1-\varepsilon)\rho_{z^M} \right] \gamma_{n-1}(z_2, z_3, \dots, z_M, i) \tag{6}
\end{aligned}$$

$$\begin{aligned}
\beta_n(z^M) &= \sum_{s_{n+1}} P_{QB}(s_{n+1}|s_n=z^M) \rho_{n+1}(s_{n+1}) \\
&= \sum_{i=0}^{2^q-1} \left[\left(\alpha \delta_{z_0, i} + \sum_{\ell=1}^{M-1} \delta_{z_\ell, i} \right) \frac{\varepsilon}{M-1+\alpha} + (1-\varepsilon)\rho_i \right] \rho_{n+1}(i, z_1, z_2, \dots, z_{M-1}). \tag{7}
\end{aligned}$$

$$U_n = \ln \left(\frac{\left((1-\varepsilon)\rho_{y_n} + \frac{\varepsilon}{M-1+\alpha} \sum_{z^M} \left(\sum_{\ell=1}^{M-1} \delta_{y_n, z_\ell} + \alpha \delta_{y_n, z_0} \right) w_n(z^M) \right)}{\left((1-\varepsilon)\rho_{\bar{y}_n} + \frac{\varepsilon}{M-1+\alpha} \sum_{z^M} \left(\sum_{\ell=1}^{M-1} \delta_{\bar{y}_n, z_\ell} + \alpha \delta_{\bar{y}_n, z_0} \right) w_n(z^M) \right)} \right). \tag{8}$$

The channel type which corrupts the codeword can be either an NBNDC-QB or a DFC. If the channel being used is the NBNDC-QB, the decoder uses the QB parameters in the channel subgraph, as the receiver is assumed to have knowledge of them, which results in a matched decoding regime. On the other hand, a mismatched decoding set-up is obtained if the underlying channel is a DFC while the decoder uses the QB model that fits the DFC (i.e., it employs the QB decoder to decode data sent over the DFC). In this case, the decoder is assumed to know the normalized

Doppler frequency, the SNR, and q for which it is able to choose the appropriate QB parameters. The latter scheme is denoted by DFC-QB, while the former is denoted by QB-QB. We expect that QB parameters selected as in [1] to minimize the Kullback-Leibler divergence rate provide a good approximation to the corresponding DFC.

We first consider the QB-QB scheme in two scenarios: in the first scenario, the QB noise model has parameters $M=2$, $\alpha=1$, $\text{Cor}_{\text{QB}}=0.5$, and $q=1$ (hard-decision) and $q=2$ (soft-decision), and in the second scenario the QB parameters

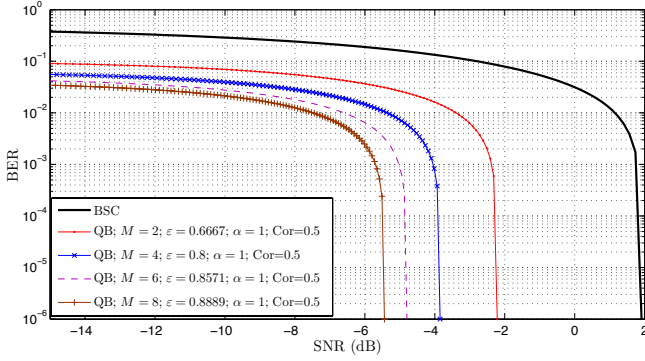


Fig. 2. SL (end-to-end BER vs SNR (in dB)) for NBNDQ-QB channels with $\text{Cor}_{\text{QB}} = 0.5$, $\alpha = 1$, $q = 1$, and $M = 2, 4, 6, 8$. Code rate $r = \frac{1}{2}$.

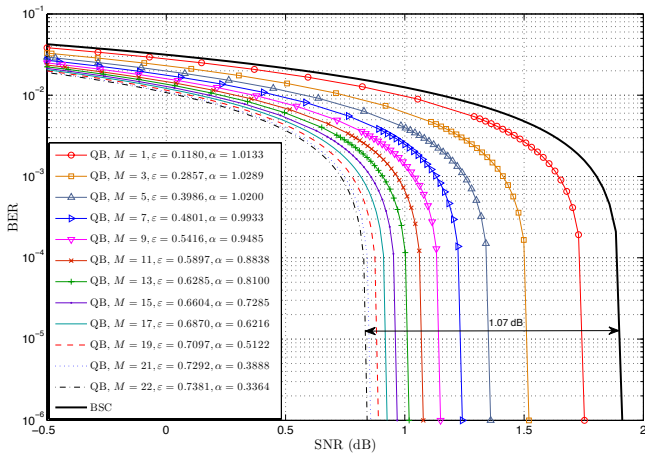


Fig. 3. SL (end-to-end BER vs SNR (in dB)) for NBNDQ-QB channels that approximate a DFC with $f_D T = 0.005$, $q = 1$, and $\text{SNR} = 1$ dB, for a code of rate $r = \frac{1}{2}$.

are $M = 3$, $\alpha = 2$, $\text{Cor}_{\text{QB}} = 0.3$, and $q = 1, 2$. The BER curves versus SNR for these two systems are shown in Figs. 4 and 5, respectively. The channels BSC and DMC correspond to perfectly interleaved channels, for $q = 1$ and $q = 2$, respectively. In Fig. 4, we observe a coding gain (at BER equal to 10^{-4}) due to only soft decision is around 2.1 dB (compare the BSC curve with the DMC one). The gain due to memory is around 3 dB (for hard decision) and 3.6 dB when we compare the DMC and NBNDQ-QB with $q = 2$. The total gain of this NBNDQ-QB with $q = 2$ relative to the BSC is around 5.8 dB. Similar coding gains are observed in Fig. 5, although they are less pronounced than in Fig. 4 as the channel's noise correlation is smaller.

Fig. 6 shows BER curves versus SNR for the transmission over a DFC with parameters $f_D T = 0.005$ and $q = 1$ under mismatched decoding, where the decoder assumes that the channel in use is an NBNDQ-QB with $M = 10$. The values of QB channel parameters α and ϵ are given in Table I for the considered range of SNR's. The BER for the BSC (the fully interleaved DFC) and the matched decoder (QB-QB) are also shown for the purpose of comparison. We remark that, while the performance is only slightly degraded by decoder mismatch vis-a-vis matched decoding, the performance is still

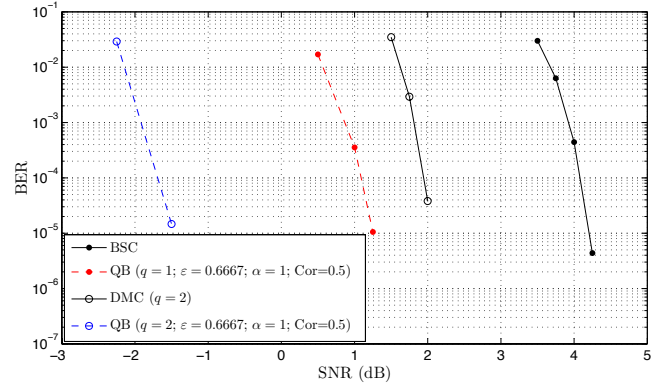


Fig. 4. End-to-end BER vs SNR (in dB) performance of LDPC codes ($N = 15000$, $K = 7500$) under matched decoding over the BSC ($q = 1$), DMC ($q = 2$), NBNDQ-QB channels (QB-QB scheme) with $\text{Cor}_{\text{QB}} = 0.5$, $M = 2$, $\alpha = 1$, and $q = 1, 2$.

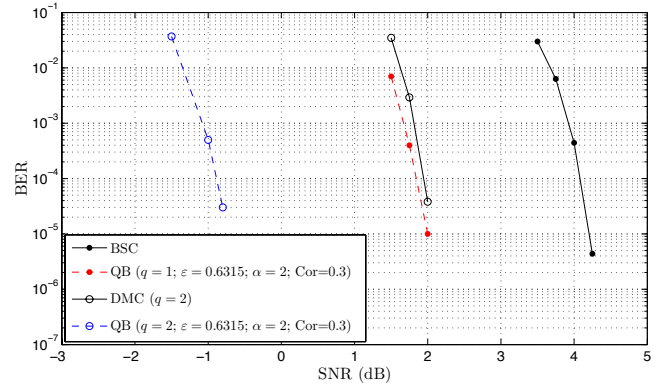


Fig. 5. End-to-end BER vs SNR (in dB) performance of LDPC codes ($N = 15000$, $K = 7500$) under matched decoding over the BSC ($q = 1$), DMC ($q = 2$), NBNDQ-QB channels (QB-QB scheme) with $\text{Cor}_{\text{QB}} = 0.3$, $M = 3$, $\alpha = 2$, and $q = 1, 2$.

better than over the memoryless BSC channel: a coding gain of about 0.57 dB is observed at a BER of 10^{-4} . A small gap of about 0.1 dB between the curves of the DFC-QB and its corresponding QB-QB scheme is observed. This indicates that the NBNDQ-QB is adequate in representing the DFC for the considered range of fading conditions.

V. CONCLUSIONS

It is shown that the NBNDQ-QB channel is effective in modeling correlated Rayleigh fading channels in terms of LDPC decoding performance. Furthermore, it is observed that when operating over such fading channels, there is a significant performance gain to be realized by exploiting the channel memory structure at the decoder (even under mismatched decoding) over the standard approach of interleaving the channel to render it memoryless and using a decoder designed for memoryless channels.

Future work includes the study of effectively reducing the complexity of the iterative decoder, which in its current form grows exponentially with the product qM of the noise memory M and soft-decision resolution q (in the case when $q = 1$, noting that the channel has a conditional block distribution

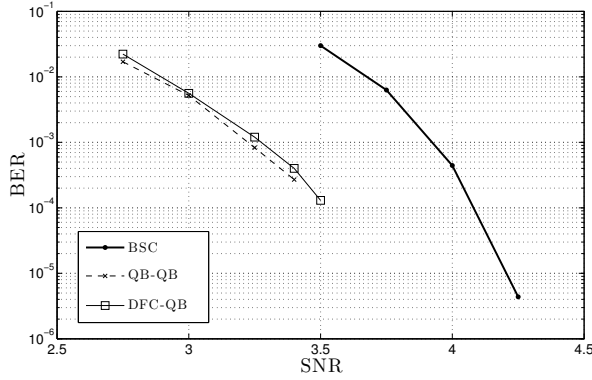


Fig. 6. End-to-end BER vs SNR (in dB) performance of LDPC codes ($N = 15000$, $K = 7500$) over the DFC with $f_D T = 0.005$ and $q = 1$. BER comparisons for the BSC (fully interleaved DFC), the DFC decoded by its QB model DFC-QB (mismatched decoding), and the QB-QB scheme (matched decoding). $M = 10$.

TABLE I
QB PARAMETERS FOR A DFC WITH $f_D T = 0.005$ AND $q = 1$.

SNR	$M = 10$	
	ε	α
2.75	0.6000	0.9038
3.0	0.6047	0.8824
3.25	0.6009	0.8763
3.4	0.6101	0.8723
3.5	0.6108	0.8705

that is linear in M promises to facilitate this endeavor) as well as comparison with reduced-complexity techniques directly developed for fading channels with memory [15]. Another interesting future direction is the construction of LDPC codes that are optimized for the NBNDQ-QB and the underlying fading channels by extending the approach of [16], [22].

REFERENCES

- [1] C. Pimentel, F. Alajaji, and P. Melo, "A discrete queue-based model for capturing memory and soft-decision information in correlated fading channels," *IEEE Trans. Commun.*, vol. 60, no. 5, pp. 1702-1711, June 2012.
- [2] W. Turin and R. van Nobelen, "Hidden Markov modeling of flat fading channels," *IEEE J. Select. Areas Commun.*, vol. 16, no. 9, pp. 1809-1817, Dec. 1998.
- [3] W. Turin, *Performance Analysis and Modeling of Digital Transmission Systems*, Kluwer Academic, 2004.
- [4] P. Sadeghi, R. A. Kennedy, P. B. Rapajic, and R. Shams, "Finite-state Markov modeling of Fading channels," *IEEE Signal Processing Magazine*, vol. 25, no. 5, pp. 57-80, Sept. 2008.
- [5] L. Zhong, F. Alajaji, and G. Takahara, "A binary communication channel with memory based on a finite queue," *IEEE Trans. Inform. Theory*, vol. 53, no. 8, pp. 2815-2840, Aug. 2007.
- [6] L. Zhong, F. Alajaji, and G. Takahara, "A model for correlated Rician fading channels based on a finite queue," *IEEE Trans. Veh. Technology*, vol. 57, no. 1, pp. 79-89, Jan. 2008.
- [7] S. Shahidi, F. Alajaji, and T. Linder, "MAP detection and robust lossy coding over soft-decision correlated fading channels," *IEEE Trans. Veh. Technology*, vol. 62, no. 7, pp. 3175-3187, Sept. 2013.
- [8] T. Wadayama, "An iterative decoding algorithm of low density parity check codes for hidden Markov noise channels," in *Proc. IEEE Int. Symp. Information Theory and Its Applications*, Honolulu, HI, Nov. 2000.
- [9] J. Garcia-Frias and J. D. Villasenor, "Turbo decoding of Gilbert-Elliott channels," *IEEE Trans. Commun.*, vol. 50, no. 3, pp. 357-363, Mar. 2002.

- [10] J. Garcia-Frias, "Decoding of low-density parity-check codes over finite-state binary Markov channels," *IEEE Trans. Commun.*, vol. 52, no. 11, pp. 1840-1843, Nov. 2004.
- [11] C. Nicola, F. Alajaji, and T. Linder, "Decoding LDPC codes over binary channels with additive Markov noise," in *Proc. Ninth Canadian Workshop on Information Theory*, Montreal, Canada, June 2005.
- [12] A. W. Eckford, F. R. Kschischang, and S. Pasupathy, "Analysis of low-density parity check codes for the Gilbert-Elliott channels," *IEEE Trans. Inform. Theory*, vol. 51, no. 11, pp. 3872-3889, Nov. 2005.
- [13] J. Chen and R. M. Tanner, "A hybrid coding scheme for the Gilbert-Elliott channel," *IEEE Trans. Commun.*, vol. 54, no. 10, pp. 1787-1796, Oct. 2006.
- [14] M. Kashyap and C. Winsted, "Decoding LDPC convolutional codes on Markov channels," *EURASIP J. Wireless Comm. Networking*, vol. 2008:729180, 2008.
- [15] G. Colavolpe, "On LDPC codes over channels with memory," *IEEE Trans. Wireless Commun.*, vol. 5, no. 7, pp. 1757-1766, July 2006.
- [16] X. Jin, A. W. Eckford, and T. E. Fuja, "LDPC codes for non-coherent block fading channels with correlation: Analysis and design," *IEEE Trans. Commun.*, vol. 56, no. 1, pp. 70-80, Jan. 2008.
- [17] Y. R. Zheng, and C. Xiao, "Improved models for the generation of multiple uncorrelated Rayleigh fading waveforms," *IEEE Commun. Lett.*, vol. 6, no. 6, pp. 256-258, June 2002.
- [18] F. R. Kschischang, B. J. Brendan, and H. A. Loeliger, "Factor graphs and the sum-product algorithm," *IEEE Trans. Inform. Theory*, vol. 47, no. 2, pp. 498-519, Feb. 2001.
- [19] T. M. Cover and J. A. Thomas, *Elements of Information Theory*, 2nd Ed. Wiley, 2006.
- [20] G.-C. Zhu, F. Alajaji, J. Bajcsy, and P. Mitran, "Transmission of non-uniform memoryless sources via non-systematic Turbo codes," *IEEE Trans. Commun.*, vol. 52, no. 8, pp. 1344-1354, Aug. 2004.
- [21] X. Y. Hu, E. Eleftheriou, and D. M. Arnold, "Regular and irregular progressive edge growth Tanner graphs," *IEEE Trans. Inform. Theory*, vol. 51, no. 1, pp. 386-398, Jan. 2005.
- [22] A. W. Eckford, F. R. Kschischang, and S. Pasupathy, "On designing good LDPC codes for Markov channels," *IEEE Trans. Inform. Theory*, vol. 53, no. 1, pp. 5-21, Jan. 2007.